Reprinted by permission from IEEE TRANSACTIONS ON ELECTROMAGNETIC COMPATIBILITY
Vol. EMC-13, No. 2, May 1971
pp. 41-44

Transient Currents Induced on a Metallic Body of Revolution by an Electromagnetic Pulse

DAVID E. MEREWETHER, MEMBER, IEEE

transient radiation, transient effects, body of revoluation

***Abstract*—A numerical technique is presented that may be used to predict the current induced on a thin metallic body of revolution excited by an electromagnetic pulse. Examples are given. Introduced here is the use of the radiation condition in a finite difference solution. This development alleviates the requirement that finite difference techniques be applied to a bounded region of space.**

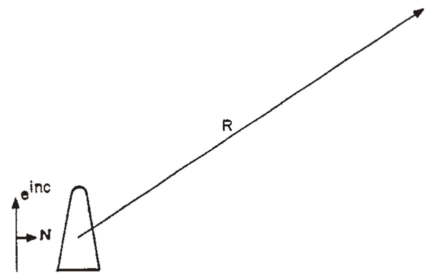

Fig. 1. Body of revolution.

INTRODUCTION

THE CURRENT induced on a metallic enclosure is interesting because it can often serve as an intermediary between an external electromagnetic field and the unwanted excitation of internal electronic circuits [1], [2]. In the study reported here a numerical solution was evolved that may be used to determine the transient current induced on a perfectly conducting body of revolution by the electromagnetic field transient generated by a lightning flash or a nuclear explosion. The finite difference formulation used here follows that developed by Yee [3] and implemented by Taylor *et al.* [4] to study the pulse scattering of a cylindrical rod in a cylindrical waveguide.

FORMULATION

The problem to be addressed is to determine the total axial current flowing on the surface of a thin body of revolution excited by an electric field transient (Fig. 1). It is assumed that the incident field is linearly polarized with the electric field vector parallel to the axis of the body.

The electromagnetic field scattered by the body satisfies Maxwell's equations at all points in space:

$$\nabla \times \boldsymbol{e} = -\mu_0 \frac{\partial \boldsymbol{h}}{\partial t} \tag{1}$$

$$\nabla \times \boldsymbol{h} = \varepsilon_0 \frac{\partial \boldsymbol{e}}{\partial t} \tag{2}$$

where $\boldsymbol{e}$ and $\boldsymbol{h}$ are scattered electric and magnetic fields and μ_0 and ε_0 are the free space permeability and permittivity, $\mu_0 = 4\pi \times 10^{-7}$ H/m and $\varepsilon_0 = 10^{-9}/36\pi$ F/m. When the antenna is thin the scattered field has azimuthal symmetry so that the curl equations (1) and (2) then reduce to the following equations:

$$\left(\frac{\partial e_r}{\partial z} - \frac{\partial e_z}{\partial r}\right) = -\mu_0 \frac{\partial h_\phi}{\partial t} \tag{3}$$

$$\left(-\frac{\partial h_\phi}{\partial z}\right) = \varepsilon_0 \frac{\partial e_r}{\partial t} \tag{4}$$

$$\left(\frac{h_\phi}{r} + \frac{\partial h_\phi}{\partial r}\right) = \varepsilon_0 \frac{\partial e_z}{\partial t}. \tag{5}$$

The nonzero components of the scattered field satisfy these equations and are subject to the boundary condition

$$e_{\tan}^{\text{total}} = e_{\tan}^{\text{inc}} + e_{\tan} = 0 \tag{6}$$

on the surface of the scatterer and the radiation condition

$$e = \frac{f(t - R/c)}{R} \tag{7}$$

at a large distance R from the center of the body (Fig. 1) where c is the velocity of light and f is some causal vector function, i.e., $f(x) = 0$, if $x \leq 0$. This system of simultaneous partial differential equations (3)–(5) can be solved subject to conditions (6) and (7) to yield the total description of the scattered field about the body.

NUMERICAL SOLUTION

Equations (3)–(5) were differenced to obtain a point centered difference formulation following Taylor *et al.* [4]:

$$h_\phi^{n+1}(i,j) = h_\phi^n(i,j) + \frac{\Delta t}{\mu_0 \Delta S}\left[e_z^n(i, j+1) - e_z^n(i,j) - e_r^n(i+1, j) + e_r^n(i,j)\right],$$
$$\text{for } 1 \leq j \leq i_{\max} \text{ and } i_{\min} < i < i_{\max} \tag{8}$$

Manuscript received November 11, 1970. This work was supported by the U.S. Air Force Weapons Laboratory.

The author is with Sandia Laboratories, Albuquerque, N. Mex. 87115.

$$e_r^{n+1}(i+1,j) = e_r^n(i+1,j) - \frac{\Delta t}{\varepsilon_0 \Delta S}[h_\phi^{n+1}(i+1,j) - h_\phi^{n+1}(i,j)],$$

$$\text{for } 1 < j < j_{\max} \text{ and } i_{\min} < i < i_{\max} - 1 \quad (9)$$

$$e_z^{n+1}(i,j+1) = e_z^n(i,j+1) + \frac{\Delta t}{2j\varepsilon_0 \Delta S}[h_\phi^{n+1}(i,j+1) + h_\phi^{n+1}(i,j)] + \frac{\Delta t}{\varepsilon_0 \Delta S}[h_\phi^{n+1}(i,j+1) - h_\phi^{n+1}(i,j)],$$

$$\text{for } 1 < j < j_{\max} - 1 \text{ and } i_{\min} < i < i_{\max} \quad (10)$$

where

$$h_\phi^n(i,j) = h_\phi(t,r,z)\Big|_{\substack{t=n\Delta t\\ z=i\Delta S\\ r=(j-1/2)\Delta S}} \quad (11)$$

$$e_r^n(i,j) = e_r(t,r,z)\Big|_{\substack{t=(n+1/2)\Delta t\\ z=(i-1/2)\Delta S\\ r=(j-1/2)\Delta S}} \quad (12)$$

$$e_z^n(i,j) = e_z(t,r,z)\Big|_{\substack{t=(n+1/2)\Delta t\\ z=i\Delta S\\ r=(j-1)\Delta S}} \quad (13)$$

where Δt and ΔS are selected time and spacial increments with $c \cdot \Delta t < \Delta S/2$. The ranges $i_{\min}$, $i_{\max}$, and $j_{\max}$ are yet to be determined.

Boundary Conditions

The presence of the body of revolution is easily introduced into the finite difference formulation by setting the field components equal to zero within the body. Since the body is assumed to be thin at the highest frequency of interest ($a_{\max} \ll \lambda_{\min}$), the shape of the body may be replaced by a discrete approximation passing through constant e_r and constant e_z surfaces (Fig. 2). On this approximate surface the boundary condition (6) is easily expressed: $e_r = 0$ on the horizontal surfaces and $e_z = -e^{\text{inc}}$ on the vertical surfaces.

From (8)–(10) it is apparent that not all the needed field components may be calculated from the difference equations. The following quantities must be supplied externally:

$$e_z^n(i,1), \qquad \text{for } i_{\min} \le i \le i_{\max} \quad (14)$$

$$e_z^n(i,j_{\max}+1), \qquad \text{for } i_{\min} \le i \le i_{\max} \quad (15)$$

$$e_r^n(i_{\min},j), \qquad \text{for } 1 \le j \le j_{\max} \quad (16)$$

$$e_r^n(i_{\max+1},j), \qquad \text{for } 1 \le j \le j_{\max}. \quad (17)$$

The first quantity (14), the z component of the electric field on the axis of the coordinate system, is merely left out of the differencing scheme. It may be approximated by

$$e_z^{n+1}(i,1) = e_z^{n+1}(i,2). \quad (18)$$

The remaining three quantities are ultimately determined by the radiation condition (7). At early times there is no need to calculate fields so far from the body that the scattered field has not yet arrived. The calculation can be limited to the region where the scattered field is nonzero by making $i_{\min}$, $i_{\max}$, and $j_{\max}$ functions of time, viz., let $i_{\text{space}} =$

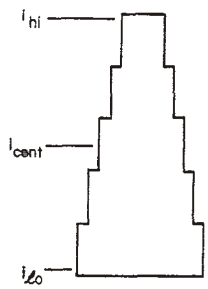

Fig. 2. Approximate body shape.

int $[c \cdot t/\Delta S + 5]$:

$$i_{\min} = i_{\text{lo}} - i_{\text{space}}$$

$$i_{\max} = i_{\text{hi}} + i_{\text{space}}$$

$$j_{\max} = j_S + i_{\text{space}}$$

where j_S is the largest integer associated with the surface of the body and int $[x]$ means the integral part of the real number x.

At some time t_M, the expanding space of interest will engulf the allotted computer storage which we shall designate by integers i_{mem} and j_{mem}. (The body should be vertically positioned in the center of the allotted storage such that $i_{\text{mem}} = (i_{\text{hi}} + i_{\text{lo}}) = 2i_{\text{cent}}$.) After time t_M the size of the space where the finite difference approximations are used is limited by the computer storage, $i_{\min} = 1$, $i_{\max} = i_{\text{mem}} - 1$, and $j_{\max} = j_{\text{mem}} - 1$. The needed components (15)–(17) may be approximated using the radiation condition (7). For example, applying (7) to (15) yields

$$R_z(i,j_{\text{mem}}) \cdot e_z^{n+1}(i,j_{\text{mem}}) = f_z\left(t_{n+1} - \frac{R_z(i,j_{\text{mem}})}{c}\right) = f_z\left(t_n - \frac{R_z(i,j_{\text{mem}}-1)}{c} + \Delta t\theta\right) \quad (19)$$

where

$$R_z(i,j) = \Delta_S\sqrt{(i-i_{\text{cent}})^2 + (j-1)^2} \quad (20)$$

$$\theta = 1 - \frac{R_z(i,j_{\text{mem}}) - R_z(i,j_{\text{mem}}-1)}{c\,\Delta t}, \quad \theta \le 1. \quad (21)$$

For fields satisfying the radiation condition (7),

$$R_z(i,j_{\text{mem}}-1) \cdot e_z^n(i,j_{\text{mem}}-1) = f_z\left(t_n - \frac{R_z(i,j_{\text{mem}}-1)}{c}\right). \quad (22)$$

Therefore, $e_z^{n+1}(i,j_{\text{mem}})$ may be obtained by parabolic interpolation between elements of the time sequence $e_z^n(i,j_{\text{mem}}-1)$, $n = 1,2,\cdots$, as follows:

$$e_z^{n+1}(i,j_{\text{mem}}) = \frac{R_z(i,j_{\text{mem}}-1)}{2R_z(i,j_{\text{mem}})} \times [\theta(\theta-1)e_z^{n-1}(i,j_{\text{mem}}-1) + 2(1-\theta^2)e_z^n(i,j_{\text{mem}}-1) + \theta(\theta+1)e_z^{n+1}(i,j_{\text{mem}}-1)]. \quad (23)$$

Formulas for the needed e_r components (16) and (17) are obtained by similar reasoning:

$$e_r^{n+1}(1,j) = \frac{R_r(2,j)}{2R_r(1,j)} [\theta(\theta - 1)e_r^{n-1}(2,j) + 2(1 - \theta^2) \times e_r^n(2,j) + \theta(\theta + 1)e_r^{n+1}(2,j)] \quad (24)$$

$$e_r^{n+1}(i_{mem},j) = \frac{R_r(2,j)}{2R_r(1,j)} [\theta(\theta - 1)e_r^{n-1}(i_{mem} - 1, j) + 2(1 - \theta^2)e_r^n(i_{mem} - 1, j) + \theta(\theta + 1)e_r^{n+1}(i_{mem} - 1, j)] \quad (25)$$

where

$$R_r(i,j) = \Delta_S\sqrt{(i - i_{cent} - 0.5)^2 + (j - 0.5)^2} \quad (26)$$

$$\theta = 1 - \frac{R_r(1,j) - R_r(2,j)}{2\,\Delta t} \quad (27)$$

and where

$$R_r(i_{mem},j) = R_r(1,j)$$

$$R_r(i_{mem} - 1,j) = R_r(2,j).$$

Accuracy of Radiation Condition Approximation

When the asymptotic form of the scattered field is used to approximate the fields a finite distance from the body an interesting question arises. How close to the body can the approximation be applied and yet obtain an accurate prediction of the current observed on the body?

Numerical data related to this question were obtained by calculating the current induced on a thin cylindrical scatterer with endcaps by an electric field unit step as shown in the following equation:

$$e^{inc}(t) = u(t) = \begin{cases} 1 \text{ V/M}, & t \geq 0. \\ 0, & t < 0. \end{cases}$$

Several calculations were made; in each succeeding calculation the use of the radiation condition approximation (23)–(25) was applied at points closer to the structure. A comparison of the current observed at the center of the cylinder (Fig. 3) reveals the surprising accuracy of the approximation.

Even for the case $r_{max} = l/2$ and $z_{max} = l$, the accuracy is adequate for most purposes. When the approximation was applied at greater distances, the inaccuracy introduced by the approximation was not detectable.

Numerical Examples

Several examples are given to illustrate how the transient electromagnetic response of a body is affected by body shape. For simplicity the incident electric field in each case is assumed to be the unit step previously described. While the unit step is an unrealistic incident field waveshape, the normalized response data calculated represents solely the characteristics of the structure: the dominant frequencies contained in the waveshape are the first few harmonics of the resonant frequency of the structure.

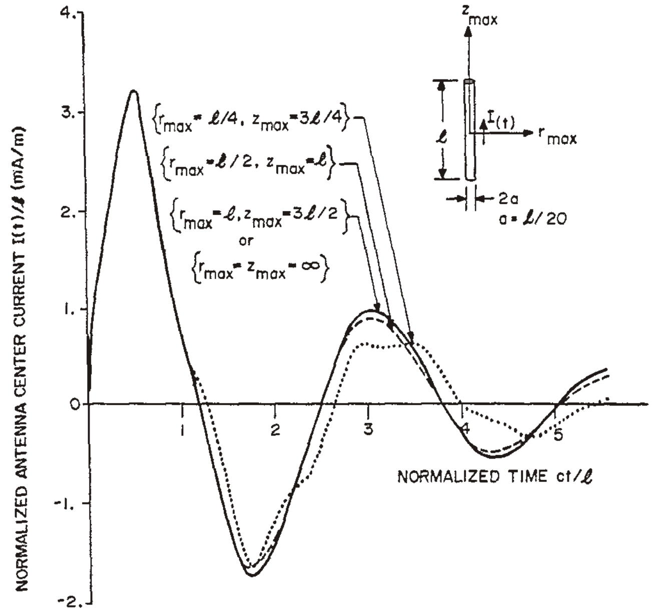

Fig. 3. Dependence of unit step response on distance that radiation condition approximation was introduced.

The first example is the truncated cone with endcaps (Fig. 4). For comparison the current observed on an endcapped cylinder with radius equal to the average radius of the cone was also calculated. Evidently very little change in the resonant frequency of the structure occurs, probably because the area of both endcaps on the conical structure is not much different from the area of both endcaps on the cylindrical structure. It is also interesting to note that at common axial locations the largest current is observed on the structure with the largest radius at that point.

As a second example, two different forms of the biconical structure (Fig. 5) were considered. The comparison of the currents induced on these structures by an electric field step illustrates the effects of body shape on the current waveshape.

It may be noted that the large endcaps on the expanding cones reduce the resonant frequency of the structure. Also, the damping of the current waves on the diminishing cones is higher than it is on the expanding cones, suggesting that the diminishing cones form a more effective radiator at high frequencies.

The current transients observed on each structure at $z = l/4$ (or $z = 3l/4$) is the same until $ct/l = 0.25$. At this time the difference in the shape of the two structures is first detectable at the point of observation.

During the early time period before reflections arrive at the center of the body, the center current induced on the expanding cones resembles a ramp function, while the center current on the diminished cones more nearly resembles the applied electric field step. This early time history is related to the fact that higher initial currents are induced on the part of the antenna with the largest radius and are propagated down the structure with little attenuation.

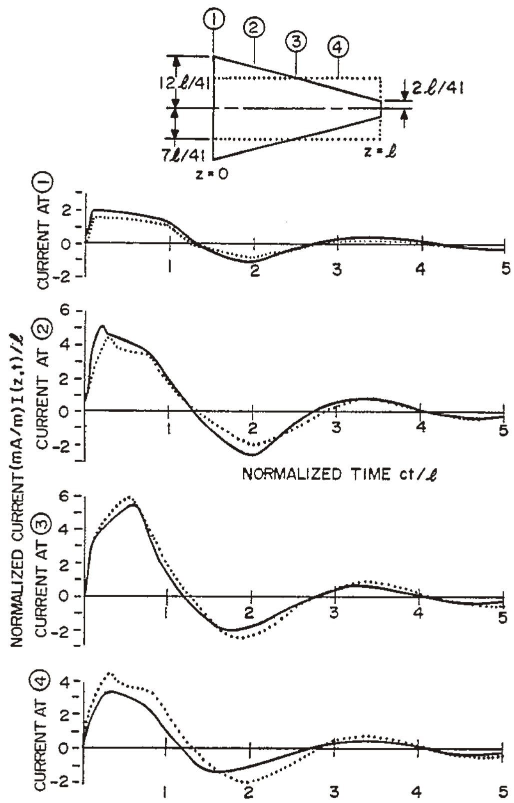

Fig. 4. Unit step response of cone and cylinder.

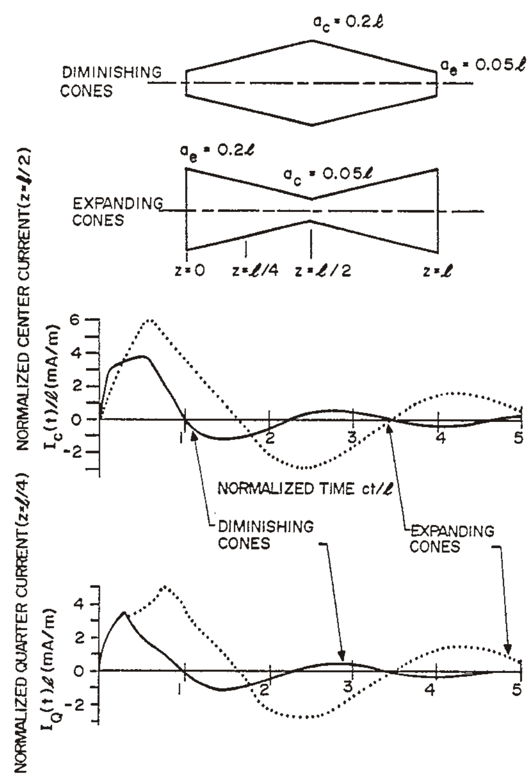

Fig. 5. Unit step response of biconical antennas.

Conclusions

In each calculation reported here the grid spacing used was reduced until the current waveforms predicted became independent of the grid spacing. Since a very fast-rising electric field step was assumed to be the input, some small-amplitude high-frequency oscillation related to the grid spacing was produced. This numerically introduced "noise" was easily isolated and removed from the data shown in this paper.

It should also be noted that the assumption that the body is thin at all significant frequencies cannot be satisfied exactly when the input electric field wave is a fast-rising unit step function. However, the dominant frequencies contained in the waveshape observed are really the first few harmonics of the resonant frequency of the structure. For these frequencies the assumption that the structure is thin is reasonable.

References

[1] C. W. Harrison, Jr., and R. W. P. King, "Response of a loaded electric dipole in an imperfectly conducting cylinder of finite length," *J. Res. Nat. Bur. Stand.*, vol. 64D, June 1960, pp. 290–291.

[2] C. W. Harrison, Jr., "Response of transmission lines in proximity to a cylindrical scatterer," *Radio Sci.*, vol. 2, Sept. 1967, pp. 1083–1091.

[3] K. S. Yee, "Numerical solution of initial boundary value problems involving Maxwell's equations in isotropic media," *IEEE Trans. Antennas Propagat.*, vol. AP-14, May 1966, pp. 302–307.

[4] C. D. Taylor, D. H. Lam, and T. H. Shumpert, "Electromagnetic pulse scattering in time-varying inhomogeneous media," *IEEE Trans. Antennas Propagat.*, vol. AP-17, Sept. 1969, pp. 585–589.